MuSCA: a multi-scale source-sink carbon allocation model to 2 explore carbon allocation in plants. An application on static apple-tree

Francesco Reyes, Benoit Pallas, Christophe Pradal, Federico Vaggi, Tagliavini Marco, Evelyne Costes, Damiano Zanotelli, Damiano Gianelle

Original Article

MuSCA: a multi-scale source-sink carbon allocation model to explore carbon allocation in plants. An application on static apple-tree structures.

F. Reyes[1,2,3,*], B. Pallas[4], C. Pradal[4,5], F. Vaggi[6], D. Zanotelli[3], M. Tagliavini[3], D. Gianelle[2], E. Costes[4]

[1] DAFNE, 01100 University of Tuscia, Viterbo, Italy, [2]DASB, CRI, Fondazione E. Mach, 38010 San Michele all'Adige, Italy, [3]Faculty of Science and Technology, Free University of Bozen-Bolzano, 39100 Bolzano, Italy, [4]AGAP, Univ. Montpellier, CIRAD, INRA, SupAgro, Montpellier, France, [5]CIRAD, UMR AGAP & Inria Zenith, Montpellier, France, [6]Amazon, 98100 Seattle, USA, [7]INRA, UMR 547 PIAF, F-63000 Clermont-Ferrand, France

Running title: MuSCA multi-scale carbon allocation model

[*]For correspondence. Email reyes.francesco@protonmail.com

ABSTRACT

Background and aims

Carbon allocation in plants is usually represented at a topological scale, specific to each model. This makes the results obtained by different models, and the impact of their scales of representation, difficult to compare. In this study, we developed a Multi Scale Carbon Allocation model (MuSCA) that allows using different, user-defined, topological scales of a plant, and assessing the impact of each spatial scale on simulated results and computation time.

Methods

Model multi-scale consistency and behavior were tested on three realistic apple tree structures. Carbon allocation was computed at five scales, spanning from the metamer (the finest scale, used as a reference) up to 1st order branches, and for different values of a sap friction coefficient. Fruit dry mass increments were compared across spatial scales and with field data.

Key Results

The model was able to represent effects of competition for carbon assimilates on fruit growth. Intermediate friction parameter values provided results that best fitted field data. Fruit growth simulated at the metamer scale differed from about 1% at growth unit scale up to 60% at first order branch and fruiting unit scales. Generally, the coarser the spatial scale the more predicted fruit growth diverged from the reference. Coherence in fruit growth across scales was also differentially impacted, depending on the tree structure considered. Decreasing the topological resolution reduced computation time by up to four orders of magnitude.

Conclusions

MuSCA revealed that the topological scale has a major influence on the simulation of carbon allocation. This suggests that the scale should be a factor which is carefully evaluated when using a carbon allocation model, or when comparing results produced by different models. Finally, with MuSCA, trades-off between computation time and prediction accuracy can be evaluated by changing topological scales.

Keywords: MuSCA, multi scale, carbon allocation, plant growth, tree growth, functional-structural plant modeling, FSPM, multiscale tree graph, source, sink, apple, plant architecture

INTRODUCTION

Carbon allocation is the process by which carbon assimilated by leaves, or stored in the form of carbohydrates, is transferred, via the conductive vessels (or phloem tissue) to other plant parts, where it is used primarily for respiration and growth. It is generally accepted that the phloem sap moves as a consequence of osmotically generated pressure gradient, as described by the Munch theory (Münch 1930). Gradients are generated by the differences in the concentrations of carbon (C) assimilates between C-sources (mainly leaves, where C-assimilates are loaded into the phloem) and sinks (where C-assimilates are unloaded from the phloem). The Münch theory has been refined over time (e.g. with the introduction of the leakage-retrieval mechanism (Thorpe *et al*. 2005) and complementary hypotheses have been proposed to explain the lack of fit with experimental evidences (e.g. sieve tubes decomposed in shorter, overlapping components, at the edge of which solutes are transported at the expense of internal energy) (De Schepper *et al*. 2013). The underlying principles, however, are still considered as valid. As such, the C-allocation process is thought to depend primarily on the amount and distribution of the available C-supplies, on demands along the plant structure and on the possibility of C-supplies to flow via the phloem (Ryan and Asao 2014). In models of small plants, however, the simplifying assumption that distance has no effect on C-availability or phloem osmotic potential (known as the 'common assimilate pool') can be made (Heuvelink 1995; Guo *et al*. 2006; Luquet *et al*. 2006; De Swaef et al. 2003).

When plant topology increases in complexity, the modeling approaches to C-allocation present in the literature can be organized in four, partly overlapping, categories (Thornley and Johnson 1990; Lacointe 2000; Le Roux *et al*. 2001; Génard *et al*. 2008): models based on empirical relationships between plant parts and/or the environment; teleonomic models representing the plant as moving towards an a priori defined specific state; source–sink driven models, in which different plant components are supposed to attract C-assimilates with different strengths and lastly transport resistance and biochemical models, which represent phloem transport as starting from osmotic gradients and biochemical conversions. The most mechanistic models, which represent osmotic flows as starting from osmotic gradients, imply complex formalizations and highly detailed plant descriptions and therefore received relatively limited attention (Bancal 2002). The modest mathematical complexity of source sink models has led to them becoming the focus of a much larger number of studies. In all cases the representation of C-allocation on large tree structures described at high resolution remains computationally intractable (Balandier *et al*. 2000; Bancal 2002).

Each model represents the plant structures, and the process of carbon allocation, at a specific scale. The choice of scale may be driven by management or research needs, by the computation

time needed for the simulations and by the resolution at which the calibration and testing data was obtained. Such scales range from the individual metamer (M) (Allen *et al*. 2005) to collections of metamers that, grouped according to criteria such as their age, position or organ type (Kang *et al*. 2008), constitute larger portions of a tree structure, such as branches, main axis or even whole plant compartments (Lakso and Johnson 1990; Kang *et al*. 2008).

By way of example, the L-PEACH model (Grossman and DeJong 1994; Allen *et al*. 2005) is a reference for completeness of the described processes and represents tree growth over multiple years. This uses a transport resistance analogy to mimic C-transport at the M scale (internode, leaf, fruit). The SIMWAL model represents the growth of a young walnut tree across several years. This is organized in axes, which are divided into growth units (GU, the scale of C-allocation), themselves composed of internodes and nodes (Balandier *et al*. 2000). A GU is an organisation level typical of plants with rhythmic growth. It corresponds to a portion of axis developed without interruption during an elongation period, and can be visually identified as bounded by two zones of scales that had protected the apical meristem in the bud during resting period. The QualiTree model represents growth and quality of fruits on a peach tree structure, at the fruiting unit (FU) scale, during a single growth season (Lescourret *et al*. 2011, Pallas et al. 2016). A FU includes the set of shoots born from a common section of one year old wood. In this model all the different types of organs in a FU are considered similar with respect to assimilates exchange, which depends on their respective distances only.

The computation of C-allocation by a model is affected by both the formalism used to describe the physiological processes and the discretization of the plant. Because of this, identifying what causes differences in results produced by different models can be difficult.

The present work proposes a new, source-sink, **Mu**lti-**S**cale **C**arbon **A**llocation model (named MuSCA), whose aim is to allow for a flexible definition of topological plant scales concomitant with the simulation of carbon allocation. The model relies on the use of Multi-scale Tree Graph (MTG) (Godin and Caraglio 1998), a formalism inspired by the observation of the multi-scale organization of plant structures (Barthélémy 1991; Barthélémy and Caraglio 2007; Balduzzi *et al*. 2017). MTG allows for the topological description of a plant at multiple, nested, spatial scales on the same graph. In addition to the connections and boundaries of the described topological scales, intensive (e.g. organ type) or extensive (e.g. geometrical features) properties can be assigned to the individual plant component at any scale. MTG has been previously used in plant architecture analyses (Costes *et al*. 2003), in radiation interception (Da Silva, Han, and Costes 2014), as well as to simulate physiological processes (Fournier *et al*. 2010; Ndour *et al*. 2017;

Barillot *et al*. 2018) or model plant-pathosystems (Garin *et al*. 2014, 2018; Robert *et al*. 2018) (albeit by using a single scale at a time).

In this paper, we provide an overview of the MuSCA model, define its scope and inputs, present the formalisms used to compute C-allocation and to move across scales. The model is calibrated for the apple tree (*Malus* x *domestica Borkh*.), Fuji cultivar, for C-demands. It is linked to a radiative model for the estimation of C-assimilates by leaves. The model is then applied on three contrasted apple tree structures and for different values of an empirical sap friction parameter, and the effects of competition for C-assimilates on fruit growth are analyzed. Field observations are then compared to the fruit growth distribution simulated on one tree structure to retain the sap friction parameter values that might best represent sap flow dynamics. The ability of the multi-scale formalism to produce similar results across scales and the influence of the scale of representation on the simulated carbon allocation are analysed. Finally, the trade-off between computational efficiency and accuracy are discussed, also in respect to the possible interactions between specific tree structure and the topological scale used.

MATERIALS AND METHODS

Model Description

Overview

MuSCA is a generic, functional structural plant model (FSPM) (Vos *et al*. 2010) representing the carbon allocation and organ growth of a plant at different, user-defined, spatial scales, while taking into account competition and distances between carbon sinks and supplies present on the plant (Fig.1). The model has a modular architecture and each module is generalized so that only a few of them are specific to a given cultivar or species (Table 1, Table 2). The model is integrated in the open-source OpenAlea environment (Pradal *et al*. 2008, 2015) and implemented in the Python language. The model reuses existing OpenAlea components, such as the MTG dynamic data-structure (Godin and Caraglio 1998; https://github.com/openalea/mtg), used to represent the multiscale topology of plant structures, the PlantGL library (Pradal *et al*. 2009) used to represent the 3D geometry, and the RATP radiative model (Sinoquet *et al*. 2001). The MuSCA model simulates biomass accumulation over a single vegetative season.

Input plant structures and creation of new scales

The input plant structures of MuSCA are MTGs where individual plant components are characterized by qualitative or quantitative information. Qualitative information refers to the organ type or the type of connection between vertex and parent (i.e. branching or succession). Quantitative information may include parameters such as the geometry or age of a plant component. This information can be used to create criteria defining the membership of individual plant components to larger groups of adjacent plant components.

Movement of carbon

The movement of the available carbon (F_{ij}), from a C-supply (i) to a C-sink (j), is represented as a function of the C-available in the supply (ACP_i), the sink C-demand ($Demand_j$) (eq. 1a), and is inversely related to the distance ($dist$) between source and sink and to a sap friction parameter (h) (eq. 1b), along the plant topology. The h factor is an empirical friction parameter, proposed in previous source-sink carbon allocation models (Balandier *et al*. 2000; Lescourret *et al*. 2011). Larger values of this parameter amplify the effects of distance resulting in relatively large amounts of C allocated next to the source, while a value of zero implies no effect of distance. This equation is inspired by a previously defined equation (SIMWAL model, Balandier *et al*. 2000).

$$F_{ij} = \frac{Demand_j * f(dist_{ij},h) * ACP_i}{\sum_{k=1}^{n} Demand_k * f(dist_{ik},h)} \qquad \textbf{(eq. 1a)}$$

$$f(dist_{ij},h) = \frac{1}{(1+dist_{ik})^h} \qquad \textbf{(eq. 1b)}$$

If in excess, the C-allocated to a plant component will just fulfill its C-demand, while the excess will be stored in a reserve pool for this compartment and be considered as a supply provided by that component on the following time-step (Balandier *et al*. 2000). However, since simulations in this study lasted for only one day, this phenomena never occurred.

The carbon allocated to a topological element is eventually divided among the different organs that constitute it (at the metamer scale: fruit, leaf, internode), proportionally to their individual carbon demand.

Calculation of distances

A representation of the C-allocation process coherent at multiple topological scales requires the definition of an equation for the calculation of distances, independent of the scale of representation.

Modeling C-allocation is computationally demanding as, in a source-sink formulation, it requires to compute the distance between all pairs of carbon sinks and sources in the tree. In a MTG, sources and sinks are represented by vertices in a tree graph. The complexity of computing the distance between all pairs is quadratic, i.e. requires around n^2 operations, for a tree of n vertices. We thus designed an algorithm, based on the multi-scale organization of plants, which allows to reduce the number of operations by reducing the number of independent plant vertices that must be compared.

Each MTG vertex (i) is characterized, among other properties, by three dimensional coordinates (basal and top), the possibility to have a parent (named i-1), and one or multiple sons (the vertex i is the son of its parent). In a MTG, a vertex at a coarser scale (I, called complex) is composed of one or more vertices at the finer scale (called components of I), as in the case of a shoot composed of several internodes.

The distance ($dist_{i,j}$) among two vertices (i, j) in a MTG depends on the sequence of vertices that connect i and j (called topological path). It corresponds to the sum of i) the semi-lengths of the extremities i and j, and ii) the length of the topological path between the bases of i and j (eq. 2a, 2b Fig.2). The semi-length of an element at different scales is computed as the distance between its base and barycenter.

In order to assess the length of this path, it is necessary to identify the Greatest Common Ancestor (GCA) of vertices i and j (Fig.2). Given the two paths connecting the tree root to i and j, the Greatest Common Ancestor of vertex i and vertex j, GCA(i,j), is identified as the vertex that is contained in both paths and that is the closest to i and j. The topological path between i and j is the union of the vertices between i and GCA(i,j) and the path between j and GCA(i,j) with GCA(i,j) (Fig.2). The length of the path ($dist_{i,j}$) is computed as the sum of the length of each of its internal elements plus the semi-lengths of its extremities, minus twice the length of the GCA (Fig.2, eq.2a). In addition, the distance between the basis of the first two elements of the path, that are directly inserted in the GCA(i,j) and are not connected with each other, is added (eq.2a). This is the case at corser scale when different ramifications are connected to the trunk at different location. When the GCA is either i or j, the length is just the sum of the length of all its internal elements plus the semi-length of its extremities (eq.2b).

$$dist_{i,j} = semilength_i + dist_{i,GCA} + dist_{j,GCA} + semilength_j - 2length(GCA) + dist(base_{son(CGA)i}, base_{son(CGA)j}) \quad \textbf{(eq. 2a)}$$

where $son(GCA)i$(resp. j) is the first descendant in the path(i,GCA(i,j)) (resp. j).

if GCA is i or j,

$$dist_{i,j} = dist_{i-1,j-1} + semilength_i + semilength_j \quad \textbf{(eq. 2b)}$$

The calculation of the spatial coordinates of the basis and barycenters depends on the scale (Fig.2B). At M scale, the basal coordinates of a vertex correspond to the top coordinates of its *parent* vertex (eq. 3a). For the basal vertex of the MTG, the only without a parent, coordinates are stored in the complex of the same vertex. Barycenter coordinates are obtained as the mean of its top and base coordinates (eq. 3b).

At coarser scales, the basal coordinates of a vertex I are the basal coordinates of its first component at the metamer scale i.e. the one whose parent does not belong to I (eq. 3c). These basal coordinates are inherited from top coordinates of its parent (see eq. 3a).

Regarding the coordinates of the barycentre of a coarse scale vertex, these are calculated as the mean of the coordinates of the barycenters of its components, weighted by their individual lengths (as in eq. 3d for the x coordinate).

At metamer scale:

$$base_i = top_{parent(i)} \quad \textbf{(eq. 3a)}$$

$$barycenter_{X,i} = \frac{top_{X,i}+base_X}{2} \quad \textbf{(eq. 3b)}$$

At coarse scales:

$\forall\ i \subseteq I \mid \text{parent}(i) \text{ not} \subseteq \text{I}$:

$$base_I = top_{parent(i)} \quad \textbf{(eq. 3c)}$$

$$barycenter_{X,I} = \frac{\sum barycenter_{X,i} * length_i}{\sum length_i} \quad \textbf{(eq. 3d)}$$

Up- and down- scaling

In MuSCA, some of the plant properties available at one scale are used to provide a description of the same properties at a coarser (up-scaling) or finer (down-scaling) scale. This is done in simulations running at coarse scales, prior and after the calculation of carbon flows, respectively by calling up- and down- scaling functions (except for the initial calculation of biomasses, see part From geometry to biomass). The up-scaling of properties such as biomass, carbon supplies and demands of plant parts is simply done by summing up the property values

stored in all the vertices that are contained within the topological boundaries of the coarser scale component. Conversely, down-scaling the same properties from a coarse scale component to its constituting elements requires some assumptions. In particular, when the carbon allocated to a coarse scale component is down-scaled, it is assigned proportionally to the relative carbon demands of its constituent elements.

Application to realistic tree structures: the case of apple (*Malus x domestica Borkh*)

In order to assess the ability of the model to simulate similar growths across multiple scales, to represent competition for C-assimilates and the effect of the scale on computation time, we applied MuSCA on different tree structures of apple trees, represented at multiple topological scales). These were MTGs of three apple trees simulated by the MAppleT architectural model (Costes *et al*. 2008). MAppleT combines markovian models for the simulation of growth unit succession and branching with a biomechanical model for axis bending. Along growth units, individual leaf area was simulated based on a logistic function and assuming different final values of leaf areas for the preformed (7 leaves) and neoformed parts of the GU (Da Silva et al., 2014a). This model was previously calibrated on Fuji cultivar (Costes et al., 2008) and so that it could be used to generate one four year old 'Fuji' tree that was used in this study. Moreover, two other trees were simulated by initiating simulations using two different sequences of lateral types along the trunk observed on trees originated from a bi-parental population, as previously proposed by Da Silva et al. (2014b). These two trees were selected within the population in order to test our C allocation model on trees displaying contrasted architectures. Simulations were run for each individual tree on a single day, so that the direct effect of changing the topological scale could be analyzed while excluding possible retroactions and cumulative effects (such as the re-use of C delivered in excess to a plant component). A partly cloudy day of late June (day of the year = 182) was chosen to drive photosynthesis. This allowed on the one hand C-limiting conditions to occur (the use of very sunny days resulted in C-allocation generally satisfying the whole fruit C-demand), and on the other hand to represent trees in which shoot elongation, and thus the creation of new internodes, ended. Initial fruit dry weight was set to be identical for all fruits and equal to 8 g (Reyes *et al*. 2016).

For the application of the carbon allocation model on tree structures, we developed a few modules containing some species specific parameters and allometric relationships (Table 1, Table 2). These were needed, firstly to convert the geometric descriptions of the trees contained in the MTGs into values of biomass (Supplementary Information: Input tree structures), and then to estimate the values of carbon demands for dry matter accumulation (see Source and Sink strengths).

Source and Sink strengths

In MuSCA, the amount of C-assimilates available from photosynthesis in individual leaves is estimated with a radiative model: RATP: (Sinoquet *et al*. 2001) integrated within the OpenAlea platform and running on MTG structures (see also Supplementary Information: Inputs of the MuSCA model). In RATP the tree structure is first discretized into voxels of user-defined size. The voxel specific mean leaf area density (turbid medium assumption) is calculated based on the plant 3D representation in space. This is then used to compute the direct and diffused PAR and NIR light intercepted in each voxel, and its related photosynthesis, every 30 minutes, across the whole day. The C-assimilation estimated per leaf unit surface is first associated to each leaf and integrated over the whole day, and then converted into dry matter uptake per leaf per day. In this study, a previous calibration of RATP for the apple trees, Fuji cultivar (Massonnet *et al*. 2006), was used.

Sink strengths were calculated as the sum of the carbon demands for dry matter accumulation into the plant structure and the carbon lost by respiration (Table 2). The first term was assumed to follow maximum potential relative growth rates. Maximum potential growth curves were obtained by fitting thermal-time-dependent gompertz functions to organ-type-specific maximum dry weights (Grossman and DeJong 1995) of proleptic and epicormic shoots, and fruits of apple Fuji trees growing in conditions where competition for carbohydrates was minimized (Reyes *et al*. 2016). Their normalized derivatives (Hunt 1982; Grossman and DeJong 1995) represent the seasonal patterns of organ type specific activities (or maximum potential relative growth rates). Regarding the old wood, the slope of a linear relationship fitted through the logarithm of the relative growth rate of the old wood biomass vs growing degree days (GDD) obtained by Reyes et al. (2016) was used. Values of sink activities of the current days were then used, together with the organ dry weight and the Growing Degree Days (GDD), to estimate the C-demand for dry matter accumulation ($DMDemand_j$) of the same day (eq.4) (Marcelis 1996) at the metamer scale.

$$DM\ Demand_j = sink\ dry\ weight * sink\ activity(GDD)_{organtype} * GDD_{day} \quad \textbf{(eq.4)}$$

Respiration was split into maintenance and growth components as proposed by Lescourret et al. (2011) and Pallas et al. (2016). The maintenance components was modeled as proportional to dry mass, a Q10 law, and a maintenance respiration parameter. Growth respiration was considered as proportional to the growth respiration coefficient and to the sum of the carbon demanded for maintenance respiration and for the dry matter increase. Parameter values provided by Pallas et al., 2016 were used.

Definition of topological scales

Five biologically relevant scales of representation of trees were used. Two of them are commonly used in MTG (metamer and growth unit) and three are newly defined (trunk, branches and shoots; 1st order branch and inter-branches; fruiting unit) (Fig.3). New scales were defined by setting criteria for the identification of edges, along the plant topology, among which all elements could be considered as belonging to the same group. The finest scale considered was the metamer (M) (or phytomer) that is composed of a node and its leaf(ves) and axillary bud(s) plus the subtending internode. This scale was considered as a reference for the representation of carbon allocation in this study. The second scale corresponds to the GU (Barthélémy 1991). The third scale corresponded to the discretization of the tree in main trunk, first order branches originating from it and the leafy shoots (Trunk, Branches and Shoots, TBS). The fourth scale corresponded to first order branches originating from the main trunk, but without considering the individual shoots separately (BR1). The fifth scale corresponded to the FU. In all scales, the root was considered as a compartment in itself.

Simulation of fruit growth

We run simulations for the three apple tree structures represented at the five topological scales defined above. In order to identify a biologically sensible value of the friction parameter (h), this was varied across a range of almost two orders of magnitude (0.5-16).

We tested the model ability to simulate competition for the available C among tree organs at M scale. This was done by analysing the growth of individual fruits in relation to both the fruit load and the carbon assimilated in the surrounding of the analysed fruit. In particular, a neighborhood of the analyzed fruit is defined as the set of metamers for which the geometrical distance between their barycenter and the barycenter of the metamer containing the fruit is lower than a given threshold. Considered a growing fruit, the ratio between the amount of C-assimilated and the number of fruits present in its neighborhood represents a comfort index with respect to the availability of C for fruit growth and the occurrence of competition with other fruits. As such, the correlation between this ratio and the simulated growth of individual fruits belonging to the same neighborhood illustrates whether fruit growth is affected by the competition for C-assimilates occurring within the area around the analysed fruit. Based on these considerations, the values of C-assimilated and the number of other fruits in the surrounding of individual fruits present on each tree was calculated for neighborhoods of incremental radii (radii of 5, 15, 25, 35, 45, 55, 65, 75, 95, 115, 135 cm) and for different friction parameters. Then, a correlation between the ratio (C-assimilated/number of fruits) and the simulated growth of individual fruits belonging to the same neighborhood was calculated for each radius and friction parameter value. Significance of the correlations was then adjusted for

multiple comparisons with the Bonferroni correction (i.e. dividing the significance level of the test, p-value = 0.05, by the number of correlations for which significance was tested: eleven distances).

Biological relevance was also tested by comparing the simulated growth on the Fuji tree structure and harvested fruit size distribution on field trees of the same age (four years old) and cultivar. Based on the assumption that fruit weight obtained in early growth stages is correlated to the fruit weight at harvest (Stanley *et al*. 2000), we compared the distributions of the normalized values of the carbon allocated in our simulations with fruit weight measured at harvest (Costes, unpublished data). Similarity among distributions was also assessed in terms of Root Mean Squared Error (RMSE) between distribution counts. Based on these results, a narrower range of friction parameter values was identified as more biologically relevant and used in further analysis.

The coherence of simulations across scales was tested by correlating the fruit growth obtained at each coarse scale with the one at M scale, used as a reference. Results obtained for equal friction parameter and same tree structure were considered together. For each coarse scale component, the average of the fruit growth obtained at M scale within the boundaries of the coarse scale component was computed. As such, a one-to-one comparison was possible between mean growth at M and other (coarser) scales. Deviations between M and the other scales were assessed visually on correlation plots, and by means of the coefficient of variation of the root mean squared error (CV RMSE).

The effect of using different topological scales on the number of plant components and on simulation time was also analyzed. All simulations were run on a computer equipped with an Intel i7-6700HQ 2.59 Ghz CPU, 8Gb RAM; OS: Windows 10 Home, 64bit.

RESULTS

Testing physiological assumptions

Relative growth rate (RGR) of shoots in the Fuji tree structure at M scale increased with the values of the friction parameter while, for fruits and old wood, it increased for h values from 0.25 to respectively 4 and 2, and then decreased until a value of 16 (Table 3). In other terms, the higher the values of the friction parameter the higher was the growth occurring close to the C-source. RGRs of old wood and shoots were comprised between normal growth observed in the field and maximum potential growth data used for calibration of sink demands (between $5.3*10^{-3}$ and $3.1*10^{-2}$ mg/g for the old wood, between 0.4 and 1.2 mg/g for shoots; Reyes *et al*. 2016). Conversely, fruit growth was between 35% and 51% lower in respect to the fruit growth observed in the normal field conditions (1.9 and 2.8 mg/g for fruits).

Simulation results at M scale show the impact of the friction parameter (h) in determining the area around an individual fruit within which this competes for C-assimilates with other fruits (Fig.4A, B). As shown by the significant correlations among fruit growth and comfort index (ratio between C-assimilated and number of fruits), the neighborhood within which fruit growth is affected by competition for C is relatively large (>0.9 m) for small values of the friction parameter (0.5 - 4). This means that the within-tree variability in fruit growth is mostly related to C-sources located far from it. In other terms, a large part of the tree structure affects the growth of each individual fruit. Conversely, for high friction parameter values (8, 16), fruit growth is affected mainly by the C provided by close leaves and possibly the competition with neighboring fruits (neighborhood < 0.9 m) (Fig.4B).

The normalized fruit dry weight simulated on the four-year old Fuji tree was compared to that of fruits measured at harvest in a two similar trees, in order to evaluate what range of the friction parameter best fit the observed fruit size distribution (Fig.4C). The lowest RMSE values were obtained with h parameter values between 4 and 16. High values, however, produced skewed distributions with variability larger than the one obtained in the field (h = 16). Conversely, for low h values (0.5, 1) distributions had a consistently lower variability than in the field. Similar variability and low RMSE values were obtained with the friction parameter values of four and eight.

C-allocation at multiple scales

Changing the scale of representation of the tree from M to coarser scales sharply decreased the number of represented topological components of the tree structures. Trees at GU, TBS, BR1 and FU scales contained respectively about 12.7%, 8.6%, 1.6%, and 1.2% the elements they had at M scale (Table 4).

Changing topological scale had also a significant impact on fruit growth. In order to ease the interpretation, and based on the above fitted values, only results for the best friction parameter values (2 <= h <= 8) are presented. Fruit growth at GU and TBS scales was more correlated to results at M scale than at coarser scales (BR1, FU) (Fig.5). Generally, in simulations at coarse scales, fruit growth predictions was lower in respect to the M scale. For instance, when running the simulations at FU scale, differences in mean fruit dry weight compared to those obtained at M scale (used in the PEACH model, Allen *et al*. 2005) went up to 60% in terms of coefficient of variation of the RMSE (Fig.6B).

As expected, multiple fruits belonging to the same coarse scale component had the same growth (size of spheres on Fig.3). This was due to the facts that that all fruits at the beginning of the simulation had identical weight and that the carbon allocated to a coarse scale component is proportionally divided according to individual metamer carbon demand. As a consequence, the

higher the resolution in representing the plant structure (Metamer > Growth Unit > TBS > 1st order Branching ≈ Fruiting Unit), the higher number of different fruit growth achieved (Fig.5). Globally, the lower the friction parameter the lower the range of fruit growth variability, in all the tree structures and at all topological scales (Fig.4C, Fig.5D). The corollary of these observations is high values of the friction parameters result in a relatively wide range of fruit growth at all scales, but with lower within-tree variability when moving from a M to a coarse scale.

Simplification of the tree structures and computation efficiency

Computation time was found as a third order polynomial function of the number of components in the plant (Supplementary Information - Fig.1). The reduction in the number of represented plant components, obtained by changing scale from M to FU (down to 0.8%) in the presented simulations, resulted in a gain in computation time of up to four orders of magnitude (down to 0.2%) (Table 4).

The reduction in computation time associated with the use of coarser scales (Table 4) corresponded to an increased discrepancy (in terms of the Coefficient of Variation of the Root Mean Squared Error: CV RMSE) in the results obtained between M and other scales (Fig.6B). Error varied from values next to zero at low friction parameters at GU scale, to values up to sixty percent for higher frictions and BR1 or GU scales, and was generally higher for higher fiction parameter values. There were however minor exceptions to this general behavior, with low friction parameter values occasionally providing slightly higher discrepancies than higher values (e.g. for h = 4 at BR1 scale in the Ap-05 and Ap-10 tree structure, in respect to h = 8).

DISCUSSION

Multi-scale coherence, impact on predictions and computation time

To our knowledge, MuSCA is the first C-allocation model that allows simulating C-allocation at multiple topological scales within a plant representation. Simulation results revealed that the model was able to produce results which are highly correlated with the M scale, especially when running at GU scale (Fig.5). As a rule of thumb, the deviation between predictions obtained at M and other scales increased when up-scaling and for increasing friction parameter values (Fig.5, Fig.6).

Differences in C allocated to fruits at M and other scales are due to two factors. Firstly, after allocation, the C received by the different plant parts belonging to a component is no longer influenced by their individual positions. As such, the model represents the effects of distances among the components at the coarse scale selected for the simulation, but not among its constituting

elements at the finer scale. Second, while the top and basal coordinates of a coarse scale component are inherited from the finer scale components present at its extremities, the coordinates of its barycentre are not. Indeed these are computed as the mean of the coordinates of its components, weighted by their individual lengths. When distances and C-flows are calculated, this generates deviations in respect to the M scale

The deviations between M and other scales were also affected by the specific plant structure (Fig.5). This is likely related to the non-linearity of the simulated process and its relation to the different discretization of the plant. In trees, the different contribution in respect to the available C of annual organs (leaves and fruits) and the presence of the moderate C-sink of woody organs may create contrasting patches in terms of C-supplies and C-sinks (Fig.4). When the tree is discretized at different scales, the distances between patches of sources and sinks and their constituting elements are modified. By changing discretization, the set of distances to which the non-linear function (eq. 1) is applied to compute C flows also changes, implying sharp differences in C-allocation. Changes are thus related to the geometry of the tree structure as well as to the specific friction parameter, as they determine the spatial domain and the impact of the C-allocation rule. In this regard, further research would be required to explore the impact of commonly applied equations for C-allocation (e.g. eq. 1, equations in Balandier *et al*. 2000; Lescourret *et al*. 2011) on tree architectures contrasting in terms of distributions of sinks and supplies in relation to their discretization.

Changing topological scale also had a strong impact on the computation time. This is an important limiting factor for the simulation of carbon allocation in complex tree structures, and consequently simulations of tree growth at high spatial detail tends to be limited to relatively young plants (Balandier *et al*. 2000; Pallas *et al*. 2016). Computation time in MuSCA closely approximates a third order polynomial function of the number of represented plant components (Supplementary Information - Fig.1), suggesting the need to reduce plant complexity to simulate plant growth with this type of source-sink model. In this study, the GU scale was able to reproduce values and fruit growth distributions almost identical to M, while saving computation time (Fig.5, Fig.6). It is possible that the optimal scale of representation may be influenced by tree size. Because of the exponential increase in tree topological complexity with tree age, relatively small variations in C-dynamics in early growth stages may have important consequences for the development of the tree structure at later stages. We propose the hypothesis that intermediate scales comprised between M and GU may further decrease the deviations in respect to M scale. We further suggest that a mixed use of high and relatively low topological resolutions, respectively for young and older trees, may optimize prediction accuracy while still allowing for simulations on mature trees.

Testing physiological assumptions

The formalization used in MuSCA to calculate C-allocation (eq. 1a) (Balandier *et al*. 2000) represented the impact of C-availability and competition among sinks, such as the fruits (Fig.4) on fruit growth variability.

RGRs at compartment level was lower range of field observations. This is due to the choice for simulations of a partly cloudy day, in which C-assimilation could limit growth, resulting in enhanced competition for C (whereas simulations in very sunny days resulted in higher growth and reduced fruit growth variability, data not shown).

In MuSCA, the considered friction parameter (h, eq. 1) is empirical and does not correspond to a clear biological process. As in previous studies, this parameter has been estimated by trial and error (Balandier *et al*. 2000). Nonetheless, the comparison between the simulated and harvested normalized fruit growth distribution suggests that h values should be between four and eight (Fig.4C). This suggests that neither a common assimilate pool (Heuvelink 1995) of carbon nor a shoot or branch autonomy (Sprugel *et al*. 1991) was adequate for accounting for assimilate partitioning within a fruit tree as observed in previous experimental studies (Walcroft *et al*. 2004; Volpe *et al*. 2008). Moreover, fluxes from parts of trees with high carbon supply to parts with a low one have already been used for modeling the within-tree variation in fruit size in peach and apple trees (Lescourret et al. 2011; Pallas et al., 2016). Nevertheless, it has also been observed that the level of shoot or branch autonomy can vary depending on the phenological date with a higher branch autonomy during summer period compared to winter (Lacointe *et al*. 2004). Further simulations and analyses with MuSCA performed by dynamically tuning the friction parameter values could help testing such behaviors.

Advantages of flexible C-allocation at multiple-scales

By making a dynamic use of MTG (Godin and Caraglio 1998) the presented model allows us modifying the type of "individual entities" considered in source-sink exchanges within a plant structure on the fly. This is also made possible by formalisms which are equally applicable at all scales (Fig.2, eq. 2, 3) and inherit, from fine to coarse scales, the spatial (coordinates of scale boundaries) and extensive (C-demands and supplies, Up- and down- scaling) properties necessary for the calculation of C-flows.

The flexibility related to the multi-scale features of the model provides several opportunities. While the topological scale typically represented in a plant models mirrors the interests of a particular group of model users, changing the scale of representation makes the model of practical interest for multiple objectives. As showed in this study, the model can be used to assess the implications of using specific scales. From our results, in most cases and for trees of this size, the

GU scale would be a robust alternative to M, while allowing much faster simulations. Comparisons of results among C-allocation models could be facilitated by adapting the scale of representation. For instance, the individual fruit growth simulated at the FU scale can be compared with results obtained by QualiTree (Lescourret *et al*. 2011).

In this study, MuSCA was applied on MTGs issued from the MAppleT architectural model (Costes *et al*. 2008). However, MTGs coming from other sources, such as the several models present in the OpenAlea environment, could also be used, given their compliance with certain prerequisites. Also, the detail in the description of the plant could be less detailed since, technically, a representation at metamer resolution is not strictly necessary. Indeed, in order to run MuSCA, the plant description should simply allow for the identification of the organ types (via the presence of leaves and fruits), their geometrical sizes (length and radiuses) and their topological connections (succession, branching). This makes the model applicable on tree structures acquired in the field by methods such as the Terrestrial Laser Scanner (TLS), followed by topological reconstruction of the plant (Raumonen *et al*. 2013; Boudon *et al*. 2014; Reyes 2016). In addition, field data collected at various topological scales might still be suitable for model testing. Indeed, by using the up- and down-scaling, results simulated at any spatial scale can be brought to the scale at which the data for validation are available.

Model limitations and further developments

MuSCA still neglects to represent some important physiological implication of the distribution of sinks along the plant topology. In particular, the influence of individual sinks present in the path between sources and sinks on the C-flow is not fully described, as in models based on an electric analogy and the L-system formalisms (Allen *et al*. 2005; Cieslak *et al*. 2011). Indeed, two identical C-sinks (D1, D2) present at the same distance from a source (S) will receive form this source an identical amount of C, no matter if along the path between S and D1 there are stronger or more abundant C-sinks than along the path between S and D2. Nevertheless, simple models as our have the advantage to require the calibration of one parameter only compared to these previous approaches.

It is important to remember that like other carbon allocation models applicable to large plant structures, MuSCA makes use of an empirical parameter (the friction parameter). In this study we identified a range of possibly sound parameter values, but more appropriate ones could be experimentally estimated from measurements of the sap flow through marked isotopic carbon (Hansen 1967), as well as measurements of fruit growth in simple tree structures with modified fruit loads.

The MuSCA model could be further refined by using the MTG properties to increase the computational efficiency without losing prediction accuracy. For instance, when running at coarse scale, the direction of origin of C-assimilates might be used to account for distance also within the boundaries of the coarse scale component.

The creation of new metamers should be included in order to allow for the simulation of plant growth during elongation and growth periods (on not-fixed structures). In addition, given the influence of pruning on the distribution and emergence of carbon sinks, the implementation of a module describing reactions to this management practice (e.g. DeJong *et al*. 2012) would significantly extend the applicability of the model to a broader range of real cases. Further, a more detailed description of the root would be the starting point to investigate water and nutrient limitations at the soil interface.

Regarding the use of MuSCA in the larger context, its generality can ease its adaptation to different species. In addition, the modular implementation of MuSCA in the OpenAlea environment facilitates the integration with other, previously developed, models, as it was the case for the connection with the MAppleT (Costes *et al*. 2008) and the RATP models (Da Silva, Han, and Costes 2014).

CONCLUSIONS

In this study we presented MuSCA, to our knowledge the first C-allocation model allowing to simulate C-allocation at multiple topological scales of representation of the plant. The presented model provides topologically-based methods to re-interpret/simplify the topological scale at which the process of carbon allocation is simulated. The simulations revealed a major impact of the topological scale, used to discretize C-sources and sinks, on the predicted C-allocation, even when other C-allocation rules (equation for C-allocation and friction parameter) were kept constant. The model can be used to identify which degree of simplification is acceptable for the representation of plant structures without compromising the accuracy in the computation of carbon allocation. It can be used on large plants, being aware of the trades-off in terms of computation time and prediction accuracy. In addition, the flexible representation of the plant topology facilitates matching the needs of different users, while using the same model. For instance, a relatively coarse scale (e.g. branch) could be more suited for a farmer interested in fruit thinning, than a fine one (e.g. metamer) that could be the target of a modeler interested in investigating the local drivers of individual fruit size variability.

ACKNOWLEDGEMENTS

We acknowledge Jerome Ngao and Marc Saudreau from UMR PIAF, INRA at Clermont-Ferrand respectively for their help in linking RATP to MAppleT and in linking MTG and RATP, in the OpenAlea platform. F. Boudon from UMR AGAP, Cirad at Montpellier, for some tips on Python coding. The authors thank also Roberto Zampedri and Mr Mauro Cavagna for field assistance, Maddalena Campi for useful discussions, and Gareth Linsmith for supervision on the English language and kinship.

FUNDING INFORMATION

This work was financed by the FIRST FEM doctoral school, which is funded by the Autonomous Province of Trento, Italy.

LITERATURE CITED

Allen MT, Prusinkiewicz P, DeJong TM. 2005. Using L-systems for modeling source-sink interactions, architecture and physiology of growing trees: the L-PEACH model. *New Phytologist* **166**: 869–880.

Balandier P, Lacointe A, Le Roux X, Sinoquet H, Cruiziat P, Le Dizès S. 2000. SIMWAL: a structural-functional model simulating single walnut tree growth in response to climate and pruning. *Annals of Forest Science* **57**: 571–585.

Balduzzi M, Binder BM, Bucksch A, *et al.* 2017. Reshaping plant biology: qualitative and quantitative descriptors for plant morphology. *Frontiers in Plant Science* **8**.

Bancal P. 2002. Source-sink partitioning. Do we need Munch? *Journal of Experimental Botany* **53**: 1919–1928.

Barillot R, Chambon C, Fournier C, Combes D, Pradal C, Andrieu B. 2018. Investigation of complex canopies with a functional–structural plant model as exemplified by leaf inclination effect on the functioning of pure and mixed stands of wheat during grain filling. *Annals of Botany* **123**: 727–742.

Barthélémy D. 1991. Levels of organization and repetition phenomena in seed plants. *Acta Biotheoretica* **39**: 309–323.

Barthélémy D, Caraglio Y. 2007. Plant architecture: a dynamic, multilevel and comprehensive approach to plant form, structure and ontogeny. *Annals of Botany* **99**: 375–407.

Boudon F, Preuksakarn C, Ferraro P, *et al.* 2014. Quantitative assessment of automatic reconstructions of branching systems obtained from laser scanning. *Annals of Botany* **114**: 853–862.

Cieslak M, Seleznyova AN, Hanan J. 2011. A functional–structural kiwifruit vine model integrating architecture, carbon dynamics and effects of the environment. *Annals of Botany* **107**: 747–764.

Costes E, Sinoquet H, Kelner JJ, Godin C. 2003. Exploring within-tree architectural development of two apple tree cultivars over 6 years. *Annals of Botany* **91**: 91–104.

Costes E, Smith C, Renton M, Guédon Y, Prusinkiewicz P, Godin C. 2008. MAppleT: simulation of apple tree development using mixed stochastic and biomechanical models. *Functional Plant Biology* **35**: 936.

Da Silva D, Han L, Costes E. 2014. Light interception efficiency of apple trees: A multiscale computational study based on MAppleT. *Ecological Modelling* **290**: 45–53.

Da Silva D, Han L, Faivre R, Costes E. 2014. Influence of the variation of geometrical and topological traits on light interception efficiency of apple trees: sensitivity analysis and metamodelling for ideotype definition. *Annals of Botany* **114**: 739–752.

Davidson RL. 1969. Effect of root/leaf temperature differentials on root/shoot ratios in some pasture grasses and clover. *Annals of Botany* **33**: 561–569.

De Schepper V, De Swaef T, Bauweraerts I, Steppe K. 2013. Phloem transport: a review of mechanisms and controls. *Journal of Experimental Botany* **64**: 4839–4850.

De Swaef T, Driever SM, Van Meulebroek L, Vanhaecke L, Marcelis LFM, Steppe K. 2013. Understanding the effect of carbon status on stem diameter variations. *Annals of Botany* **111:** 31-46

DeJong TM, Negron C, Favreau R, *et al.* 2012. Using concepts of shoot growth and architecture to understand and predict responses of peach trees to pruning. *Acta Horticulturae*: 225–232.

Fournier C, Pradal C, Louarn G, *et al.* 2010. Building modular FSPM under OpenAlea: concepts and applications In: Davis, CA, United States, 109–112.

Garin G, Fournier C, Andrieu B, Houlès V, Robert C, Pradal C. 2014. A modelling framework to simulate foliar fungal epidemics using functional–structural plant models. *Annals of Botany* **114**: 795–812.

Garin G, Pradal C, Fournier C, Claessen D, Houlès V, Robert C. 2018. Modelling interaction dynamics between two foliar pathogens in wheat: a multi-scale approach. *Annals of Botany* **121**: 927–940.

Génard M, Dauzat J, Franck N, *et al.* 2008. Carbon allocation in fruit trees: from theory to modelling. *Trees* **22**: 269–282.

Godin C, Caraglio Y. 1998. A multiscale model of plant topological structures. *Journal of Theoretical Biology* **191**: 1–46.

Grechi I, Vivin Ph, Hilbert G, Milin S, Robert T, Gaudillère J-P. 2007. Effect of light and nitrogen supply on internal C:N balance and control of root-to-shoot biomass allocation in grapevine. *Environmental and Experimental Botany* **59**: 139–149.

Grossman YL, DeJong TM. 1994. PEACH: a simulation model of reproductive and vegetative growth in peach trees. *Tree Physiology* **14**: 329–345.

Grossman YL, DeJong TM. 1995. Maximum fruit growth potential and seasonal patterns of resource dynamics during peach growth. *Annals of Botany* **75**: 553–560.

Guo Y, Ma Y, Zhan Z, *et al.* 2006. Parameter optimization and field validation of the functional–structural model GREENLAB for maize. *Annals of Botany* **97**: 217–230.

Hansen P. 1967. 14C-Studies on Apple Trees. II. Distribution of Photosynthates from Top and Base Leaves from Extension Shoots. *Physiologia Plantarum* **20**: 720–725.

Heuvelink E. 1995. Dry matter partitioning in a tomato plant: one common assimilate pool? *Journal of Experimental Botany* **46**: 1025–1033.

Hunt R. 1982. *Plant growth curves: the functional approach to plant growth analysis*. London: Edward Arnold.

Kang M, Evers JB, Vos J, de Reffye P. 2008. The derivation of sink functions of wheat organs using the GREENLAB model. *Annals of Botany* **101**: 1099–1108.

Lacointe A. 2000. Carbon allocation among tree organs: a review of basic processes and representation in functional-structural tree models. *Annals of Forest Science* **57**: 521–533.

Lacointe A, Deleens E, Ameglio T, *et al.* 2004. Testing the branch autonomy theory: a 13C/14C double-labelling experiment on differentially shaded branches. *Plant, Cell and Environment* **27**: 1159–1168.

Lakso AN, Johnson RS. 1990. A simpified dry matter production model for apple using automatic programming simulation software In: *Acta Horticulturae*.141–148.

Le Roux X, Lacointe A, Escobar-Gutiérrez A, Le Dizès S. 2001. Carbon-based models of individual tree growth: a critical appraisal. *Annals of Forest Science* **58**: 469–506.

Lescourret F, Moitrier N, Valsesia P, Génard M. 2011. QualiTree, a virtual fruit tree to study the management of fruit quality. I. Model development. *Trees* **25**: 519–530.

Lobet G, Pound MP, Diener J, *et al.* 2015. Root system markup language: toward a unified root architecture description language. *Plant Physiology* **167**: 617–627.

Luquet D, Dingkuhn M, Kim H, Tambour L, Clement-Vidal A. 2006. EcoMeristem, a model of morphogenesis and competition among sinks in rice. 1. Concept, validation and sensitivity analysis. *Functional Plant Biology* **33**: 309–323.

Marcelis LFM. 1996. Sink strength as a determinant of dry matter partitioning in the whole plant. *Journal of Experimental Botany* **47**: 1281–1291.

Massonnet C, Regnard JL, Costes E, Sinoquet H, Ameglio T. 2006. Parametrization of the functional-structural model for apple trees. Application to simulate photosynthesis and transpiration of fruiting branches In: *Acta Horticulturae*. Denmark: ISHS, .

Münch E. 1930. *Die Stoffbewegunen in der Pflanze*. Jena.

Ndour A, Vadez V, Pradal C, Lucas M. 2017. Virtual plants need water too: functional-structural root system models in the context of drought tolerance breeding. *Frontiers in Plant Science* **8**.

Pallas B, Da Silva D, Valsesia P, *et al.* 2016. Simulation of carbon allocation and organ growth variability in apple tree by connecting architectural and source–sink models. *Annals of Botany* **118**: 317–330.

Pradal C, Boudon F, Nouguier C, Chopard J, Godin C. 2009. PlantGL: a Python-based geometric library for 3D plant modelling at different scales. *Graphical models* **71**: 1–21.

Pradal C, Dufour-Kowalski S, Boudon F, Fournier C, Godin C. 2008. OpenAlea: a visual programming and component-based software platform for plant modelling. *Functional Plant Biology* **35**: 751.

Pradal C, Fournier C, Valduriez P, Cohen-Boulakia S. 2015. OpenAlea: scientific workflows combining data analysis and simulation. *ACM SSDBM* **15**: 11–17.

Raumonen P, Kaasalainen M, Åkerblom M, *et al.* 2013. Fast automatic precision tree models from terrestrial laser scanner data. *Remote Sensing* **5**: 491–520.

Reyes F. 2016. Carbon allocation of the apple tree: from field experiment to computer modelling. PhD Thesis, University of Bolzano, Italy.

Reyes F, DeJong T, Franceschi P, Tagliavini M, Gianelle D. 2016. Maximum growth potential and periods of resource limitation in apple tree. *Frontiers in Plant Science* **7**.

Robert C, Garin G, Abichou M, Houlès V, Pradal C, Fournier C. 2018. Plant architecture and foliar senescence impact the race between wheat growth and Zymoseptoria tritici epidemics. *Annals of Botany* **121**: 975–989.

Ryan MG, Asao S. 2014. Phloem transport in trees. *Tree Physiology* **34**: 1–4.

Sinoquet H, Le Roux X, Adam B, Ameglio T, Daudet FA. 2001. RATP: a model for simulating the spatial distribution of radiation absorption, transpiration and photosynthesis within canopies: application to an isolated tree crown. *Plant, Cell and Environment* **24**: 395–406.

Sprugel DG, Hinckley TM, Schaap W. 1991. The theory and practice of branch autonomy. *Annual Review of Ecology and Systematics* **22**: 309–334.

Stanley CJ, Tustin DS, Lupton GB, Mcartney S, Cashmore WM, Silva HND. 2000. Towards understanding the role of temperature in apple fruit growth responses in three geographical regions within New Zealand. *The Journal of Horticultural Science and Biotechnology* **75**: 413–422.

Thornley JHM, Johnson IR. 1990. *Plant and crop modelling*. NY: The Blackburn Press.

Thorpe M, Minchin P, Gould N, McQueen J. 2005. 10 - The stem apoplast: a potential communication channel in plant growth regulation In: Zwieniecki MA, ed. Physiological Ecology. *Vascular Transport in Plants*. Burlington: Academic Press, 201–220.

Volpe G, Lo Bianco R, Rieger M. 2008. Carbon autonomy of peach shoots determined by 13C-photoassimilate transport. *Tree Physiology* **28**: 1805–1812.

Vos J, Evers JB, Buck-Sorlin GH, Andrieu B, Chelle M, de Visser PHB. 2010. Functional–structural plant modelling: a new versatile tool in crop science. *Journal of Experimental Botany* **61**: 2101–2115.

Walcroft AS, Lescourret F, Genard M, Sinoquet H, Le Roux X, Dones N. 2004. Does variability in shoot carbon assimilation within the tree crown explain variability in peach fruit growth? *Tree Physiology* **24**: 313–322.

Fig.1: Conceptual workflow of the model: (A) General framework for the application of the model; (B) the core of MuSCA. (A): A multi-scale tree graph representing a plant structure at a given developmental stage is provided. This is used, together with the Growing Degree Days (GDD), allometric relationships and plant geometric information to compute initial volumes and biomasses of plant components at metamer (M) scale. Carbon demands are estimated at metamer scale by making use of species specific seasonal sink activities, biomasses and GDD at the current time step. The position of individual leaves on the plant structure is used by the radiative model RATP to compute light interception and, together with meteorological conditions, the individual leaf photosynthesis. (B): The workflow follows different paths depending on the selected scale: M scale (solid lines) and coarser scales (dashed lines). The scale at which the plant is represented determines up- and down-scaling processes. In case a coarse scale is chosen, carbon demands and supplies are up-scaled. Carbon allocation is then computed among the plant components at the chosen scale. After allocation, if the selected scale was a coarse one, the carbon allocated to each component is divided among its constituent elements. Biomass of individual elements is eventually updated prior to moving to the next time-step. MTG: Multi-scale Tree Graph. In *italics* are the steps containing species specific parameters.

Fig.2: Workflow and graphical representation of the calculation of distances. (A) Workflow for the calculation of the distance between two vertices i, j: top coordinates of vertices are used to compute coordinates of basis and barycenters for the whole topology. Given two vertices i, j, their distance is calculated in three steps: the Greatest Common Ancestor (GCA) of i, j is identified; an iterative process sums the length of the vertices connecting GCA to i and j; the semi-lengths of i and j are also summed. (B) Graphical representation of the: calculation of coordinates of basis and barycenters at (above) metamer (M) scale. The base of a vertex corresponds to the top of its parent; coordinates of the barycentre of a vertex are calculated from the ones of its top and base. (Middle) the base of a coarse scale vertex (capital I) corresponds to the base of its first component (lowercase i), which is inherited from the top of its parent at M scale (lowercase i-1); coordinates of the barycenter of a coarse scale vertex are obtained as the mean ofthe coordinates of its own components at M scale, weighted by their lengths. (Below) calculation of the semi-length of a vertex, identification of GCA and computation of distances along a path connecting two vertices i, j. Data used as input of calculations are indicated by red rhombi and are connected by arrow to the respective output represented by green crosses.

Fig.3: Simulation of carbon allocation and fruit growth on a tree structure represented at different spatial scales during one day. Upper panels: tree parts represented with the same color belong to the same scale, i.e. trees with an higher number of colors are made of a higher number of components. The number of components at each scale is indicated in the corresponding low left corner. Lower panels: the volume of the represented spheres is proportional to the normalized increment in fruit dry weight within the tree. Simulations were run with a friction parameter equal to eight.

Fig.4: Physiological responses in simulations at M scale, in respect to different tree structures and friction parameters (h). A: Three dimensional representation of the tree structures with fruit growth (obtained with h parameter equal to 8). B: correlation between individual fruit growth and the ratio between carbon assimilated and number of fruits evaluated in neighborhoods of increasing radiuses. C: Distributions of the normalized simulated fruit growth (red, coloured bars) superposed with the normalized fruit dry weight measured at harvest (black, empty bars), in the 4 years old simulated and observed Fuji trees for different friction parameters. The Root Mean Squared Error (RMSE) between distribution counts for different friction parameters is provided. The upper parts of the histograms for $h < 2$ are cut off in order to allow better visualization of results on the vertical axis.

Fig.5: Mean daily fruit dry weight increment and its distribution (in Fuji apple cultivar) depending on the topological scales (from left to right), tree structure (from top to bottom) and friction parameters h (symbols). Correlation between carbon allocated to fruits per day at the selected coarse scale (y axes) vs carbon allocated to fruits per day at M scale and averaged for all metamers belonging to a same component at coarser scale (x axis) in A: Fuji, B: Ap-05, C: Ap-10. D: Fruit growth distribution in the Fuji tree structure (dashed for h=2, dotted for h=4, solid for h=8).

Fig.6: Trade-off between computation time and prediction error. The logarithm of the computation time and the Coefficient of Variation of the Root Mean Squared Error (CV RMSE) between fruit growth at different topological scales in respect to the M scale, on three tree structures and for different friction parameters (h). A: Fuji, B: AP-05, C: AP-10.

Supplementary Information - Fig.1: Computation time in respect to the number of represented structure components.

Table 1: Model parameters and equation for estimation of biomasses.

Parameter	Description	**Value/range**	**Unit**
dry_mass_to_C_mass	Ratio to convert carbon assimilated into biomass uptake	2.105263158	-
wood_density	Old wood density	700	Kg/m3
spec_leaf_surface	Per unit surface leaf dry mass	0.08	Kg/m2
dry_to_fresh_DWratio	Ratio to convert apple fruit fresh to dry weight	0.15	-
shoot_to_root_growth	Vegetative shoot to root biomass ratio	4.5	-

Generalized linear model to estimate shoot biomass (g) from length (cm) and termal time (°C)	
Dry weight = exp (a + b * log(length) + c * GDD + d * length + e * log (length * GDD))	
a	-3.073409537
b	0.706724497
c	5.78E-05
d	0.020013707
e	9.81E-05

Table 2: Model parameters and equations for the estimation of carbon demand for dry matter increase

Parameter	Description	Value/range	Unit
trunk_activity	Sink activity for old wood	0.000031	g * g^-1 * C^-1
leaf_activity	Range of values for leaf activity (from Look Up Table)	0 to $1.9*10^{\wedge-3}$	g * g^-1 * C^-1

Gompertz equation for fruits and shoots
Dry weight = a * exp(b * exp(c * GDD)

Normalized derivative
Relative Growth Rate = (a * b * c * exp(b * (exp(c * GDD)) + c * GDD))/ (a * exp(b * exp(c * GDD))

Parameters	Fruit	Proleptic shoot
A	63.703	2.406
B	-4.896	-2.84
C	-0.00104	-0.00165

GDD: Growing degree days after bloom, after cutoff of base temperature of 4.5 °C.

Table 3: Relative growth rate at metamer scale for different friction parameter values (h) on the Fuji apple cultivar. Figures are reported with five decimals in order to see RGR differences when using different h values.

Relative growth rate (mg g^{-1} dd^{-1})			
h	Old wood	Shoot	Fruit
0.25	0.016	0.50	1.19
0.5	0.016	0.50	1.20
1	0.018	0.50	1.20
2	0.019	0.51	1.22
4	0.018	0.54	1.23
8	0.015	0.63	1.17
16	0.009	0.63	0.93

Table 4: Number of components included in tree structures at different scales.

Tree structure	Scale	Number of components	%	Computation time (min)	%
Fuji	M	3355	100	175.6	100.0
	GU	521	15.5	1.0	0.6
	TBS	320	9.5	0.6	0.4
	BR1	29	0.9	0.4	0.2
	FU	67	2	0.4	0.2
Ap-05	M	4579	100	313.8	100.0
	GU	535	11.7	1.5	0.5
	TBS	402	8.8	1.1	0.4
	BR1	115	2.5	0.7	0.2
	FU	36	0.8	0.7	0.2
Ap-10	M	4083	100	246.4	100.0
	GU	449	11	1.1	0.4
	TBS	302	7.4	0.8	0.3
	BR1	59	1.4	0.6	0.2
	FU	36	0.9	0.6	0.2

Supplementary Information

Supplementary Information: Inputs of the MuSCA model.

Variable	Description	Unit
Multi-scale Tree Graph description of a plant (.mtg)		
XX, YY, ZZ	Coordinates of the centre of the top of a plant component	m
radius	tree component apical radius	m
leaf_area	leaf area surface	m^2
fruit	fresh fruit biomass	Kg
observation	organ type: trunk, other types	-
Topological connector	">" for succession; "+" for branching	-
Scale boundary	"/" for boundary across scales	
Meteorological file for the RATP model (.mto)		
day	day of the year	day
hour	index of the current semi-hour from midnight	30 min
PARglob	global incident Photosynthetically Active Radiation	W m^-2
PARdif	diffused Photosynthetically Active Radiation	W m^-2
NIRglob	global incident Near Infrared Radiation	W m^-2
NIRdif	diffused Near Infrared Radiation	W m^-2
Ratmos	Total incoming radiation	W m^-2
Tsol	mean soil temperature	°C
Tair	mean air temperature	°C
Eair	H2O partial pressure	Pa
CO2air	CO2 partial pressure	Pa
Wind	wind speed above tree	m s^-1

Supplementary Information: Input tree structures

In the current application, input tree structures were MTGs produced by the MAppleT model (Costes *et al*. 2008). MAppleT includes (i) Markov models for simulating annual shoot branching and successive growth across years, (ii) a biomechanical model simulating the change in branch form over time, and (iii) a modified pipe-model to estimate axis radial growth. The leaf area and internode length depend on their rank along the shoot (Da Silva, Han, and Costes 2014). The MTGs output produced by MappleT are apple trees structures at a certain stage of development (given date of the year), represented at two scales, the growth unit and metamer. Metamer attributes are its apical and basal 3D coordinates, stem diameter, leaf area and fruit weight (if present).

At the beginning of the simulation, the model uses the geometrical description of the plant and some species specific parameters (Reyes *et al*. 2016, in-field observations) to estimate the initial dry weight of each plant component at the metamer scale (see Supplementary Information: Inputs of the MuSCA model). In particular: dry weight of old wood and vegetative internodes are computed as functions of their geometrical description (lengths and radiuses), and of a constant (wood density) or a function of thermal time, respectively; fruits dry weight is calculated from fresh weight and a constant (dry to fresh fruit dry weight ratio); leaf dry weight is calculated from surface and a constant (per unit surface leaf dry mass) (Table 1). Dry mass of individual internodes is calculated as follows: volumes of internodes are first computed as truncated cones, summed up to provide the volume of individual shoots and stored at a "current year shoot" coarse scale. The length of current year shoots is then obtained by summing the lengths of their internodes, and used to estimate shoot biomass by means of a thermal-time dependent allometric relationship (Table 1) (Reyes *et al*. 2016). Finally, the dry biomass of individual internodes is calculated as their individual volumetric fraction in the shoot to which they belong, multiplied by the shoot dry biomass.

Regarding the root, a rough representation of this compartment was added to the plant. A root mass, defined as proportional to the total mass of the current year shoots, is added to the root metamer following the shoot/root functional balance assumption (Davidson 1969; Grechi *et al*. 2007). The length of the roots is represented as equal to half the average distance between the soil and the vegetative shoots. The root basal coordinates are thus defined equal to the tree basal coordinates, except for the vertical (z axis) component, to which the calculated distance is subtracted (downward translation).

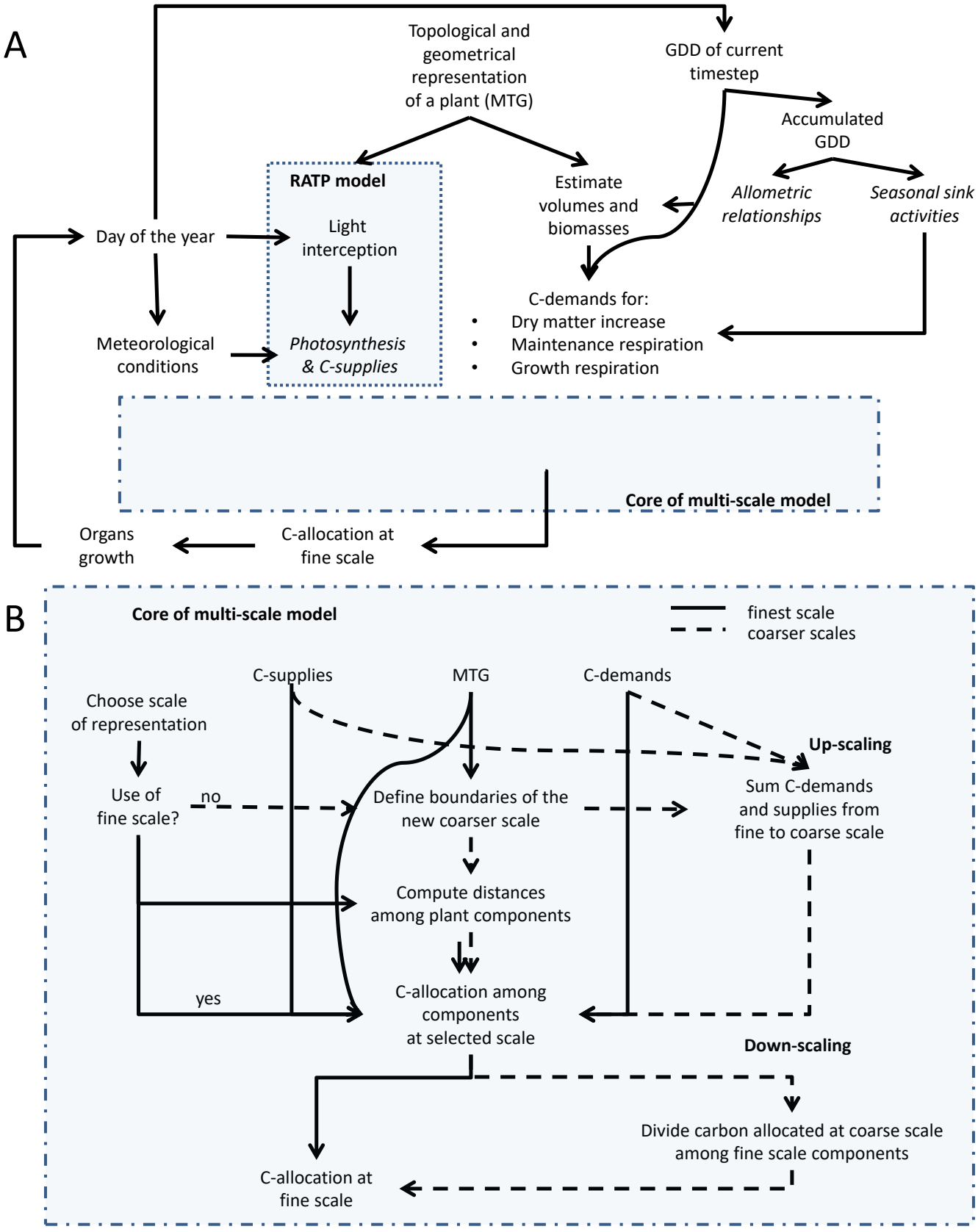
A
Topological and geometrical representation of a plant (MTG)
GDD of current timestep
Accumulated GDD
Allometric relationships
Seasonal sink activities
RATP model
Estimate volumes and biomasses
Day of the year
Light interception
Meteorological conditions
Photosynthesis & C-supplies
C-demands for:
• Dry matter increase
• Maintenance respiration
• Growth respiration
Core of multi-scale model
Organs growth
C-allocation at fine scale
B
Core of multi-scale model
finest scale
coarser scales
C-supplies
MTG
C-demands
Choose scale of representation
Up-scaling
Use of fine scale?
no
Define boundaries of the new coarser scale
Sum C-demands and supplies from fine to coarse scale
Compute distances among plant components
yes
C-allocation among components at selected scale
Down-scaling
Divide carbon allocated at coarse scale among fine scale components
C-allocation at fine scale

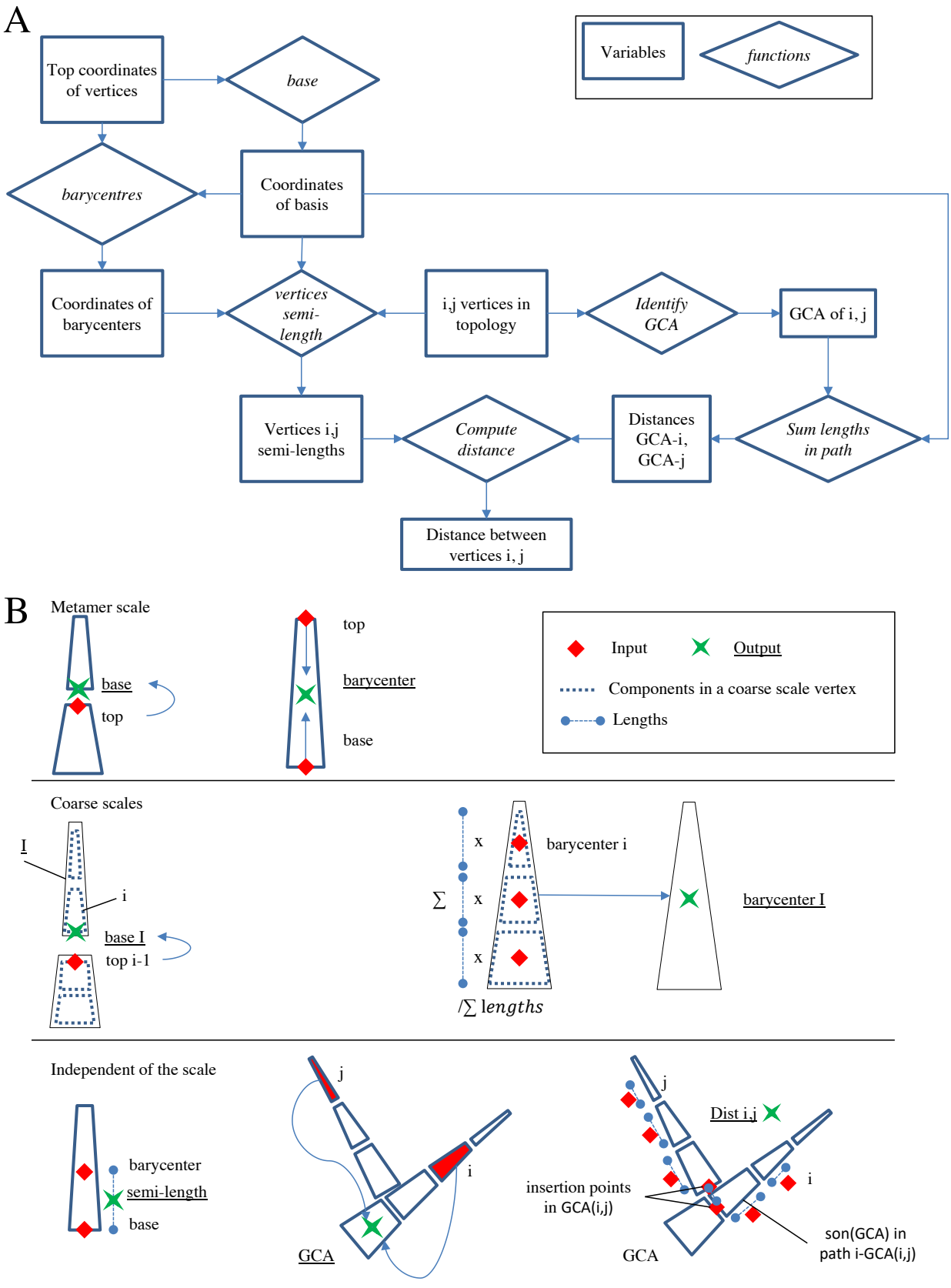
A
Top coordinates of vertices
base
Variables
functions
barycentres
Coordinates of basis
Coordinates of barycenters
vertices semi-length
i,j vertices in topology
Identify GCA
GCA of i, j
Vertices i,j semi-lengths
Compute distance
Distances GCA-i, GCA-j
Sum lengths in path
Distance between vertices i, j
B
Metamer scale
base
top
top
barycenter
base
Input
Output
Components in a coarse scale vertex
Lengths
Coarse scales
I
i
base I
top i-1
x
x
x
∑
barycenter i
barycenter I
/∑ lengths
Independent of the scale
barycenter
semi-length
base
j
i
GCA
j
Dist i,j
i
insertion points in GCA(i,j)
GCA
son(GCA) in path i-GCA(i,j)

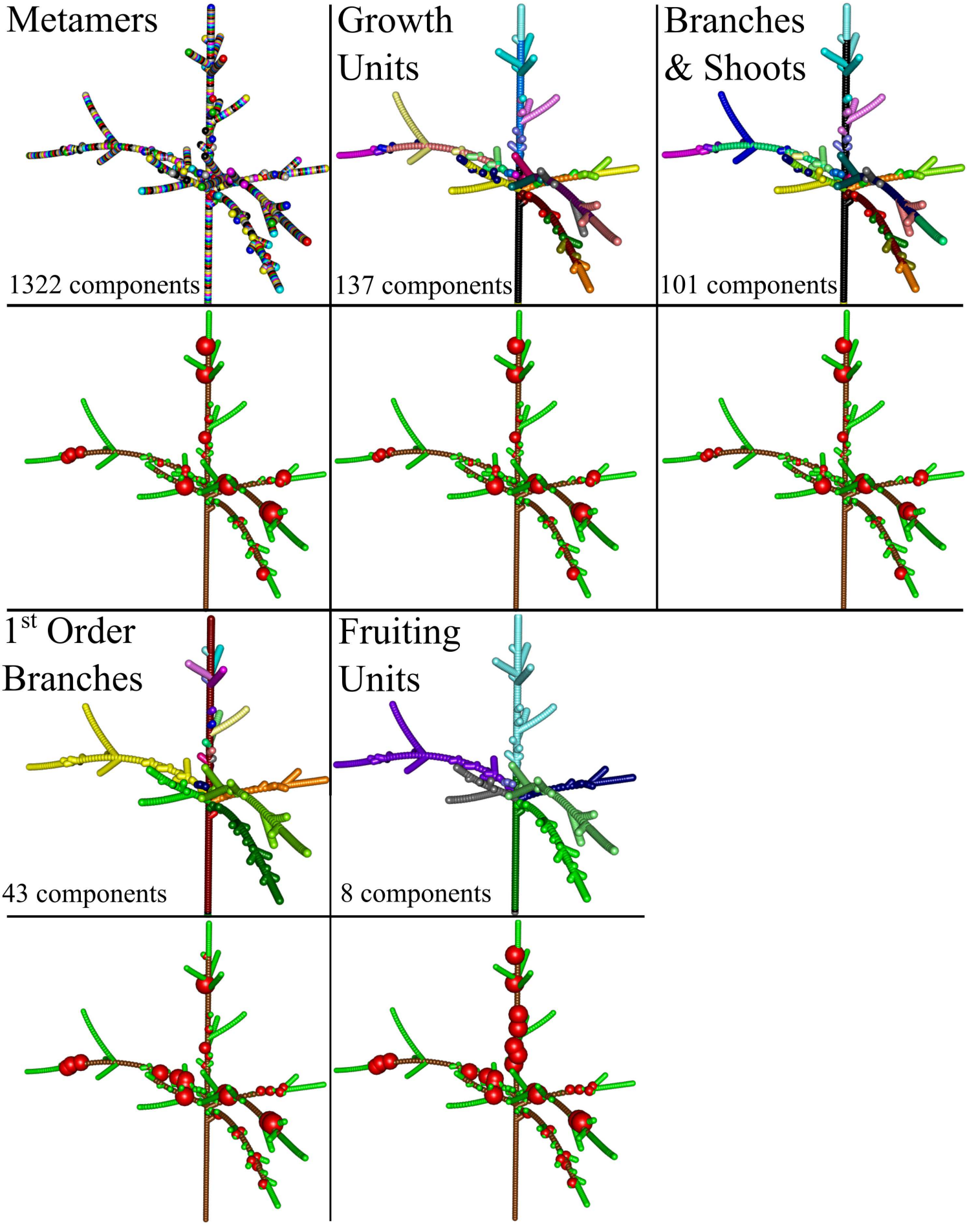
Metamers
1322 components
Growth Units
137 components
Branches & Shoots
101 components
1st Order Branches
43 components
Fruiting Units
8 components

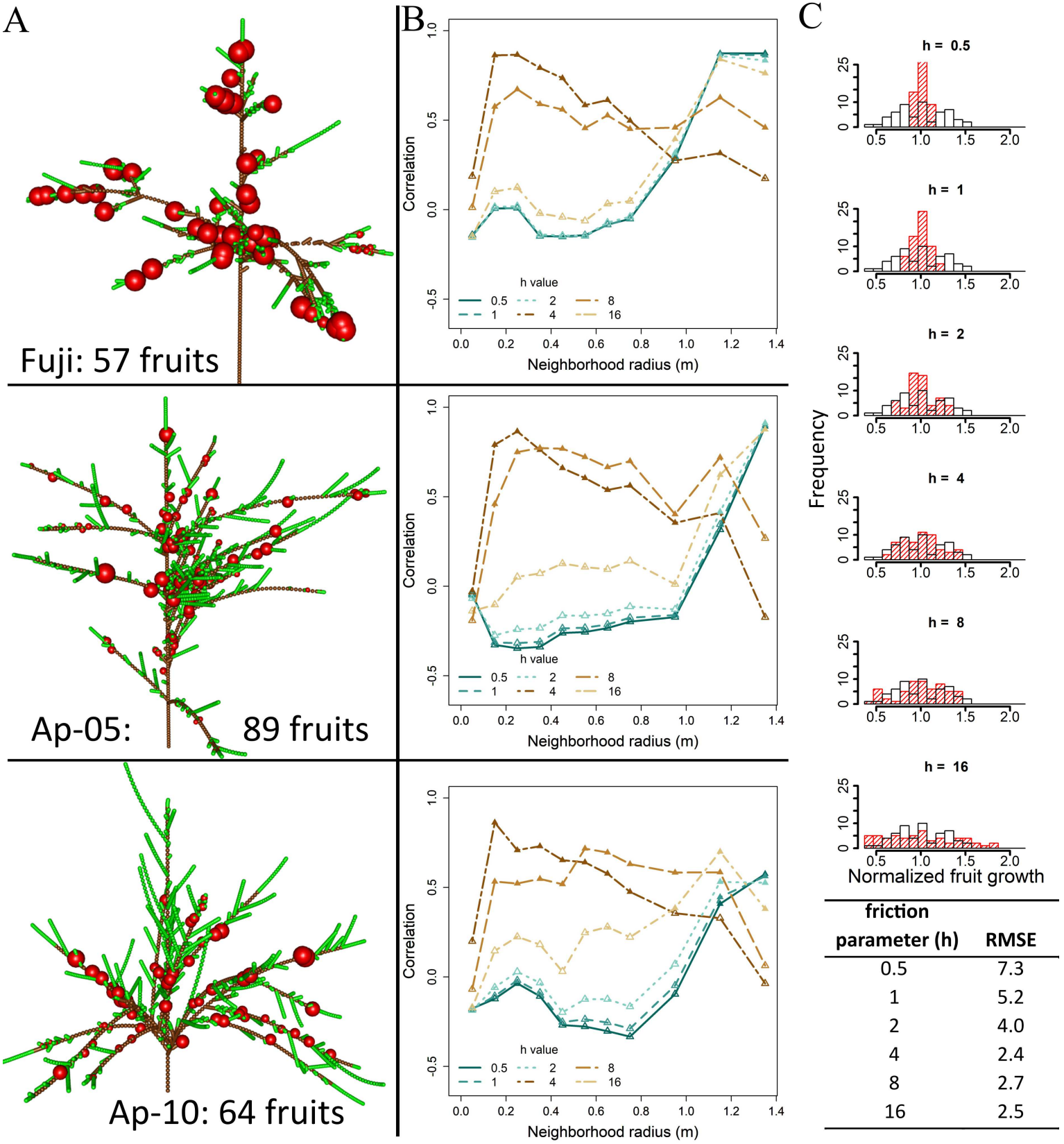

friction parameter (h)	RMSE
0.5	7.3
1	5.2
2	4.0
4	2.4
8	2.7
16	2.5

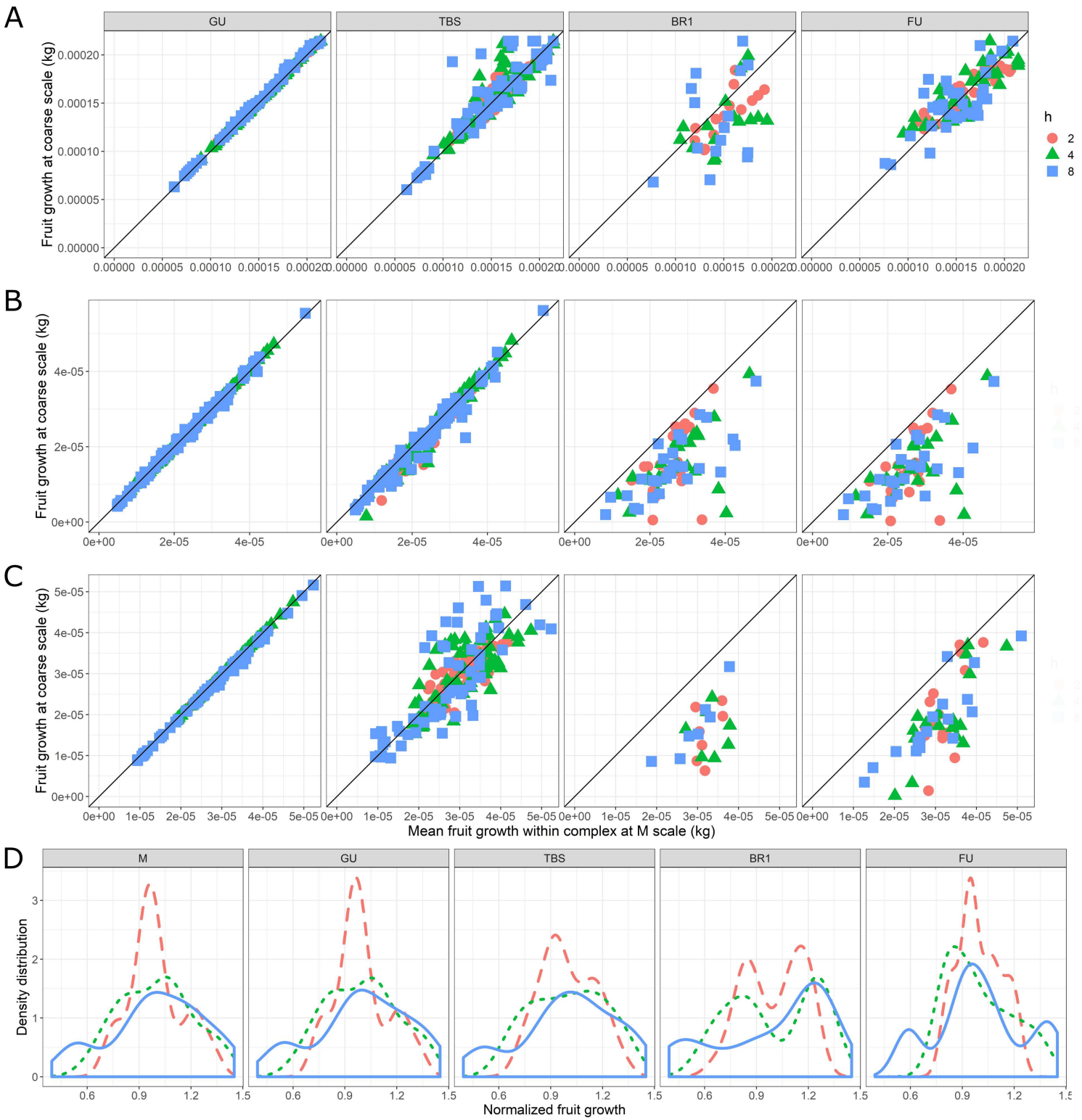
A
GU
TBS
BR1
FU
Fruit growth at coarse scale (kg)
0.00000
0.00005
0.00010
0.00015
0.00020
h
2
4
8
B
Fruit growth at coarse scale (kg)
0e+00
2e-05
4e-05
C
Fruit growth at coarse scale (kg)
0e+00
1e-05
2e-05
3e-05
4e-05
5e-05
Mean fruit growth within complex at M scale (kg)
D
M
GU
TBS
BR1
FU
Density distribution
0
1
2
3
0.6
0.9
1.2
1.5
Normalized fruit growth

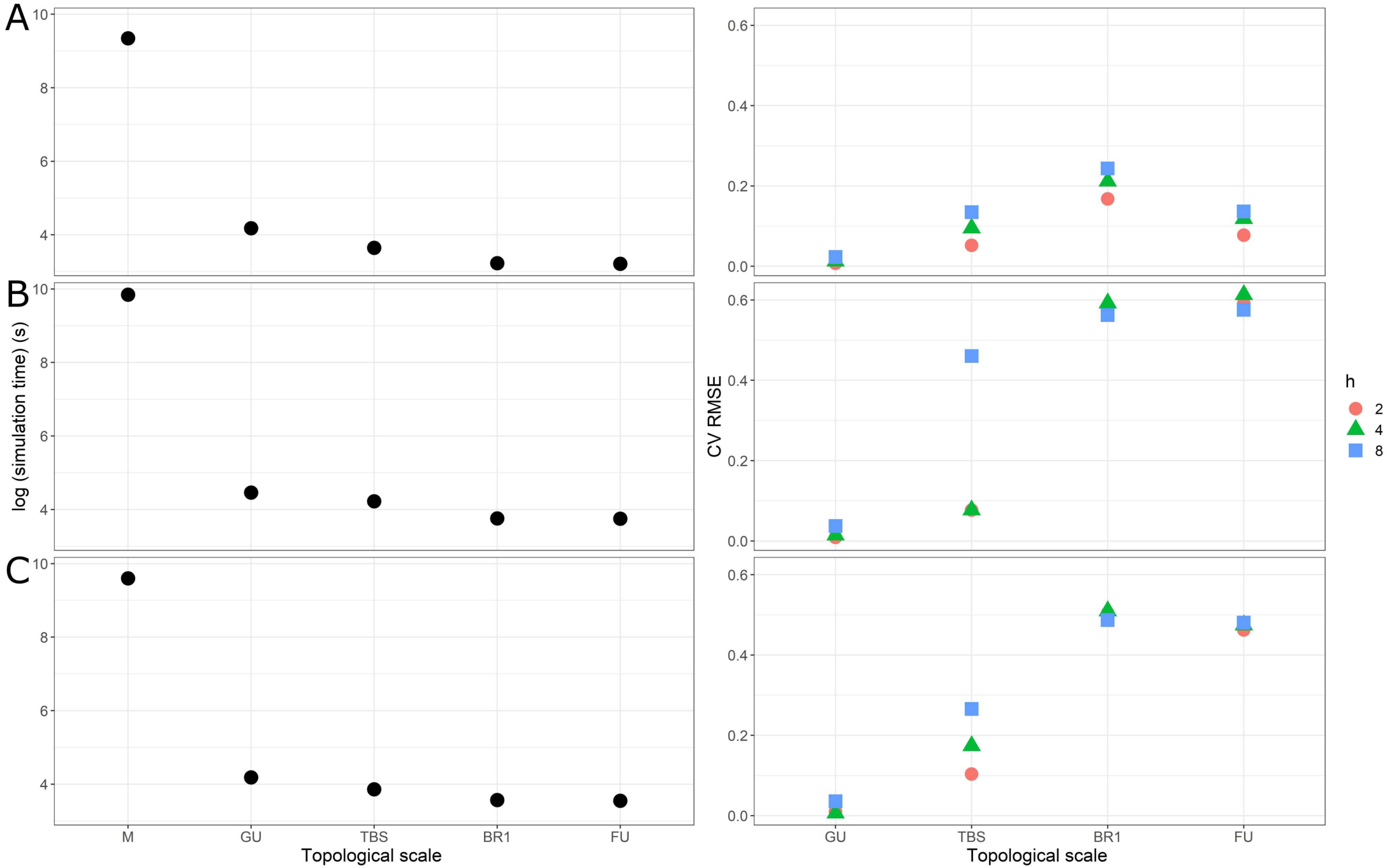
A
B
C
log (simulation time) (s)
10
8
6
4
M
GU
TBS
BR1
FU
Topological scale
CV RMSE
0.6
0.4
0.2
0.0
GU
TBS
BR1
FU
Topological scale
h
2
4
8